ISCI, Volume *3*

Supplemental Information

Ubiquitous Flame-Retardant Toxicants Impair Spermatogenesis in a Human Stem Cell Model

Alyse N. Steves, Joshua M. Bradner, Kristen L. Fowler, Danielle Clarkson-Townsend, Brittany J. Gill, Adam C. Turry, W. Michael Caudle, Gary W. Miller, Anthony W.S. Chan, and Charles A. Easley IV

Supplemental Figures and Legends

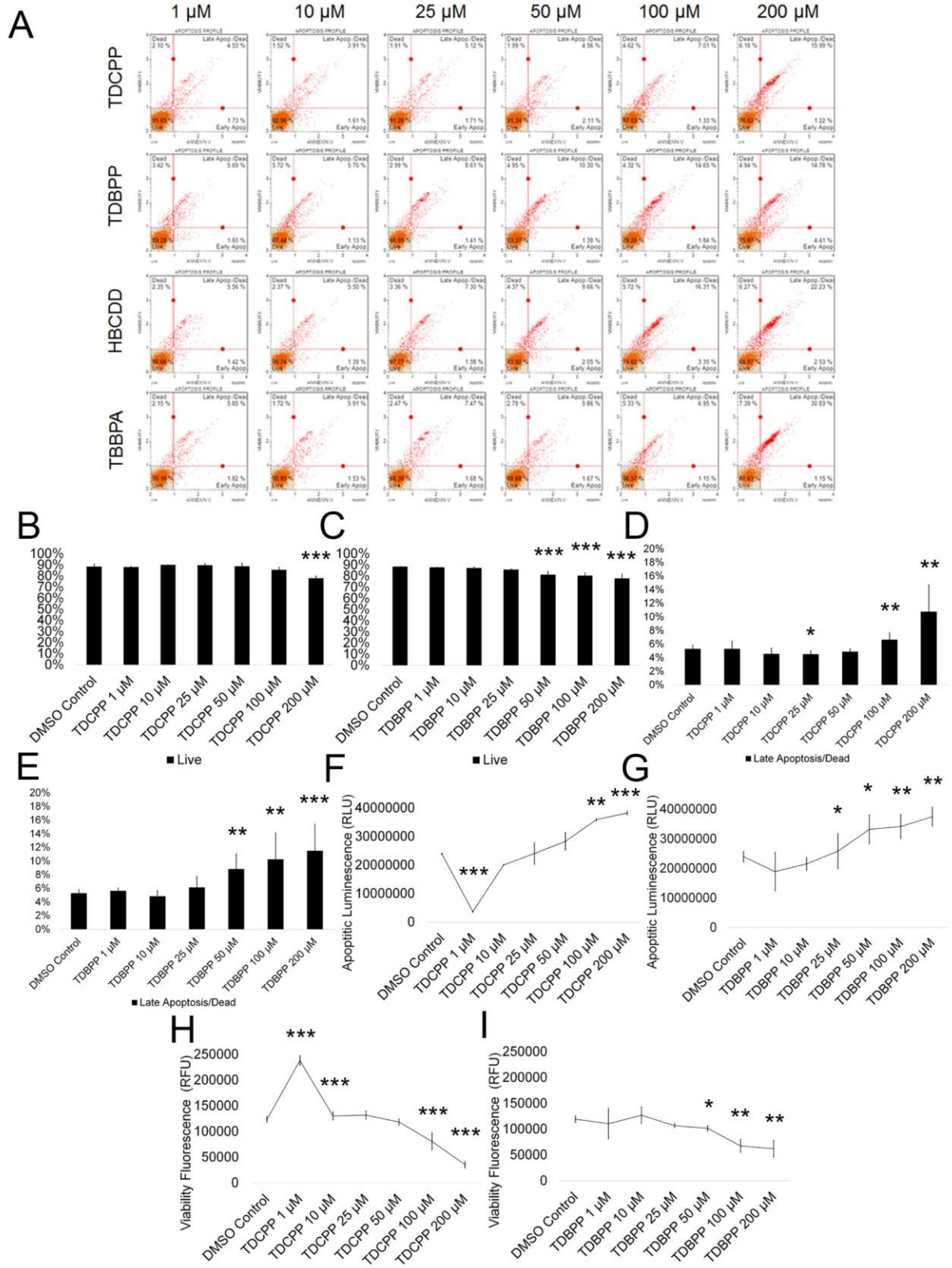

Figure S1. Related to Figure 1. TDCPP, TDBPP, HBCDD and TBBPA induce apoptosis in spermatogenic cells derived from hESCs. (A) Flow cytometry analyses indicating percent viable cells, percent early apoptotic cells, percent late apoptotic cells, and percent dead/necrotic cells for all concentrations of TDCPP, TDBPP, HBCDD, and TBBPA assessed. Lower left quadrant represents viable cells, lower right quadrant represents early apoptotic cells, upper right quadrant is late apoptotic/dead cells, and the upper left quadrant is dead/necrotic cells. (B-C) Graphical representation showing that TDCPP and TDBPP decrease germ cell viability in hESCs differentiated in *in vitro* spermatogenic conditions. (D-E) Graphical representation showing that TDCPP and TDBPP increase the percentage of germ cells undergoing late apoptosis/death in spermatogenic cells derived from hESCs. (F-G) Graphical representation showing that TDCPP and TDBPP increase apoptotic luminescence in hESCs differentiated in *in vitro* spermatogenic conditions. (H-I) Graphical representation showing that TDCPP and TDBPP decreased viability fluorescence in hESCs differentiated in *in vitro* spermatogenic conditions. 5,000 events were analyzed, with five replications performed for each condition for A-E. Three replications were analyzed for F-I. Significant changes in cell viability were determined using a 1-way analysis of variance (1-way ANOVA) and validated via a Student's t-test, where * is $p<0.05$, ** is $p<0.01$, and *** is $p<0.001$. Data are represented as mean ± SEM.

Impacts of HBCDD and TBBPA Exposure on Spermatogenesis

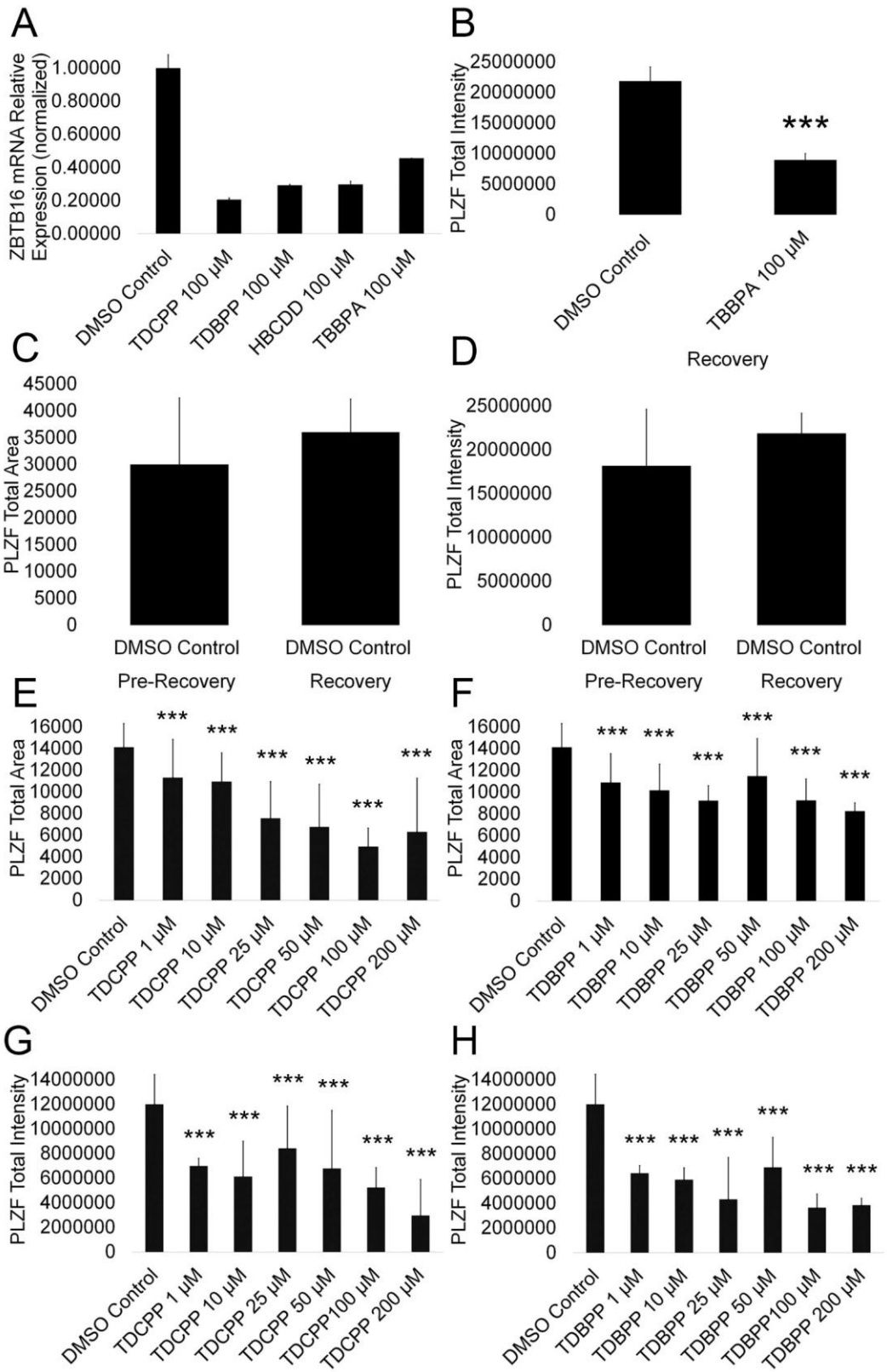

Figure S2. Related to Figure 2. TDCPP, TDBPP, HBCDD, and TBBPA exposure impact PLZF expression. (A) mRNA steady state transcripts for ZBTB16 (PLZF) correspond to decreases in PLZF+ area and intensity in immunostaining data for TDCPP, TDBPP, HBCDD, and TBBPA. (B) Graphical representation showing that PLZF intensity in spermatogonia derived under *in vitro* spermatogenic conditions treated with TBBPA remain below control levels following a twenty-four hour, chemical-free recovery period. (C) Graphical representation showing that PLZF area in spermatogonia derived under *in vitro* spermatogenic control conditions remain statistically the same after a twenty four hour recovery period. (D) Graphical representation showing that PLZF intensity in spermatogonia derived under *in vitro* spermatogenic control conditions remain statistically the same after a twenty four hour recovery period. (E-F) Graphical representation showing that TDCPP and TDBPP reduce average PLZF+ area in spermatogonia derived under *in vitro* spermatogenic conditions. (G-H) Graphical representation showing that TDCPP and TDBPP reduce average PLZF+ intensity in spermatogonia. mRNA transcript levels were normalized to 0.2% DMSO-only control. Two separate replications were performed in duplicate (n=4) for each condition. Significant changes in mRNA steady state levels were determined using Bio-Rad CFX Manager™ Software (Bio-Rad, Hercules, CA). Five replications were performed for each condition for PLZF immunostaining for E-H. Three replications were performed for B-D. Significant changes in PLZF+ area and intensity were determined using a 1-way analysis of variance (1-way ANOVA) and validated via a Student's t-test, where * is $p<0.05$, ** is $p<0.01$, and *** is $p<0.001$. Data are represented as mean ± SEM.

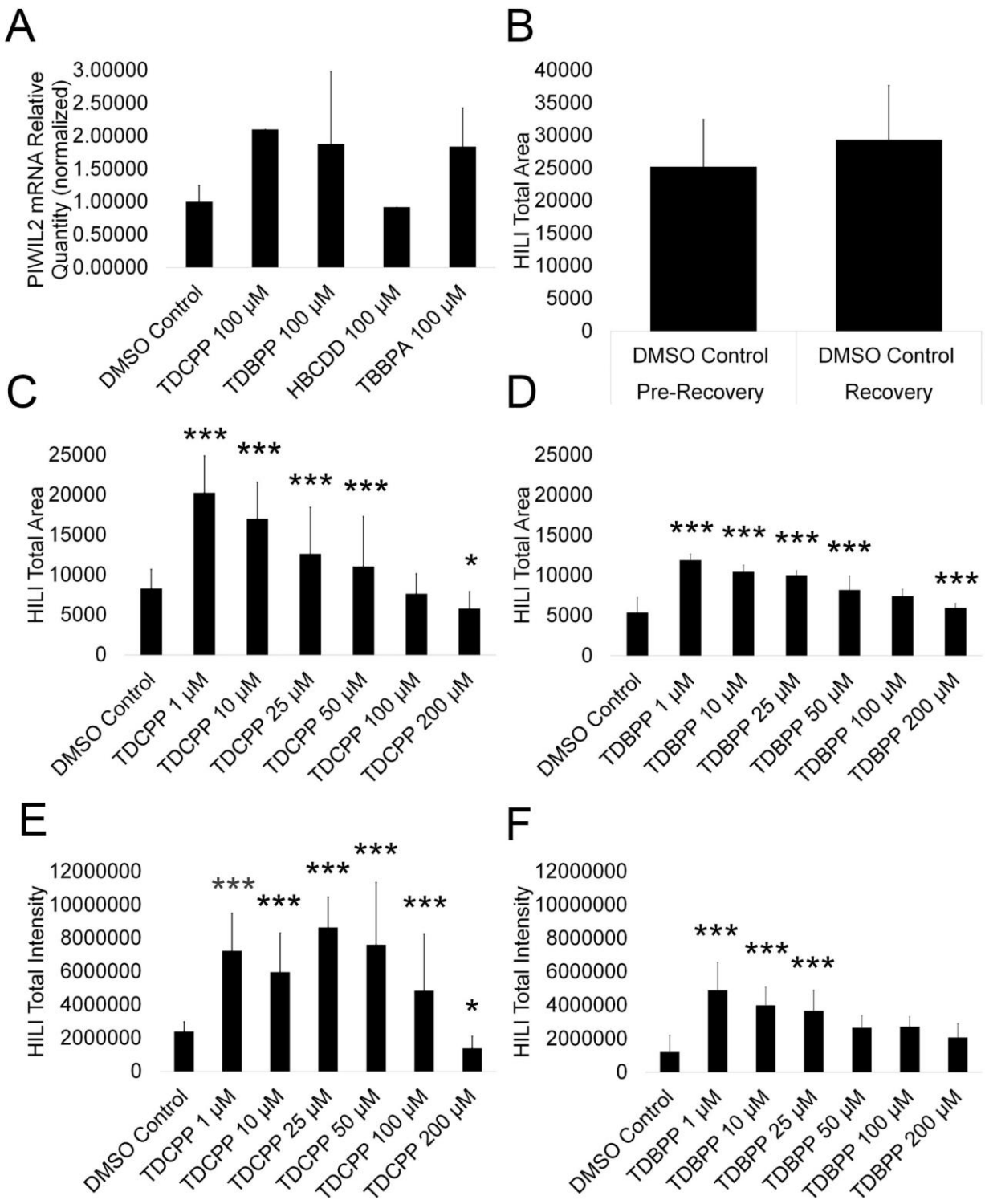
A
PIWIL2 mRNA Relative Quantity (normalized)
3.00000
2.50000
2.00000
1.50000
1.00000
0.50000
0.00000
DMSO Control
TDCPP 100 µM
TDBPP 100 µM
HBCDD 100 µM
TBBPA 100 µM
B
HILI Total Area
40000
35000
30000
25000
20000
15000
10000
5000
0
DMSO Control
Pre-Recovery
DMSO Control
Recovery
C
HILI Total Area
25000
20000
15000
10000
5000
0
***
***
***
***
*
DMSO Control
TDCPP 1 µM
TDCPP 10 µM
TDCPP 25 µM
TDCPP 50 µM
TDCPP 100 µM
TDCPP 200 µM
D
HILI Total Area
25000
20000
15000
10000
5000
0
***
***
***
***
***
DMSO Control
TDBPP 1 µM
TDBPP 10 µM
TDBPP 25 µM
TDBPP 50 µM
TDBPP 100 µM
TDBPP 200 µM
E
HILI Total Intensity
12000000
10000000
8000000
6000000
4000000
2000000
0
***
***
***
***
***
*
DMSO Control
TDCPP 1 µM
TDCPP 10 µM
TDCPP 25 µM
TDCPP 50 µM
TDCPP 100 µM
TDCPP 200 µM
F
HILI Total Intensity
12000000
10000000
8000000
6000000
4000000
2000000
0
***
***
***
DMSO Control
TDBPP 1 µM
TDBPP 10 µM
TDBPP 25 µM
TDBPP 50 µM
TDBPP 100 µM
TDBPP 200 µM

Figure S3. Related to Figure 3. TDCPP, TDBPP, HBCDD, and TBBPA exposure impact HILI expression. (A) mRNA steady state transcripts for PIWIL2 (HILI) correspond to increases in HILI+ area and intensity in immunostaining data corresponding to certain concentrations of TDCPP, TDBPP, HBCDD, and TBBPA. (B) Graphical representation showing that HILI area in primary spermatocytes derived under *in vitro* spermatogenic control conditions remain statistically the same after a twenty four hour recovery period. (C-D) Graphical representation showing that TDCPP and TDBPP impact average total HILI+ area in primary spermatocytes derived under *in vitro* spermatogenic conditions. (E-F) Graphical representation showing that TDCPP and TDBPP impact average total HILI+ intensity in primary spermatocytes. mRNA transcript levels were normalized to 0.2% DMSO-only control. Two separate replications were performed in duplicate (n=4) for each condition. Significant changes in mRNA steady state levels were determined using Bio-Rad CFX Manager™ Software (Bio-Rad, Hercules, CA). Five replications were performed for each condition for HILI immunostaining for C-F. Three replications were performed for B. Significant changes in HILI+ area and intensity were determined using a 1-way analysis of variance (1-way ANOVA) and validated via a Student's t-test, where * is $p<0.05$, ** is $p<0.01$, and *** is $p<0.001$. Data are represented as mean ± SEM.

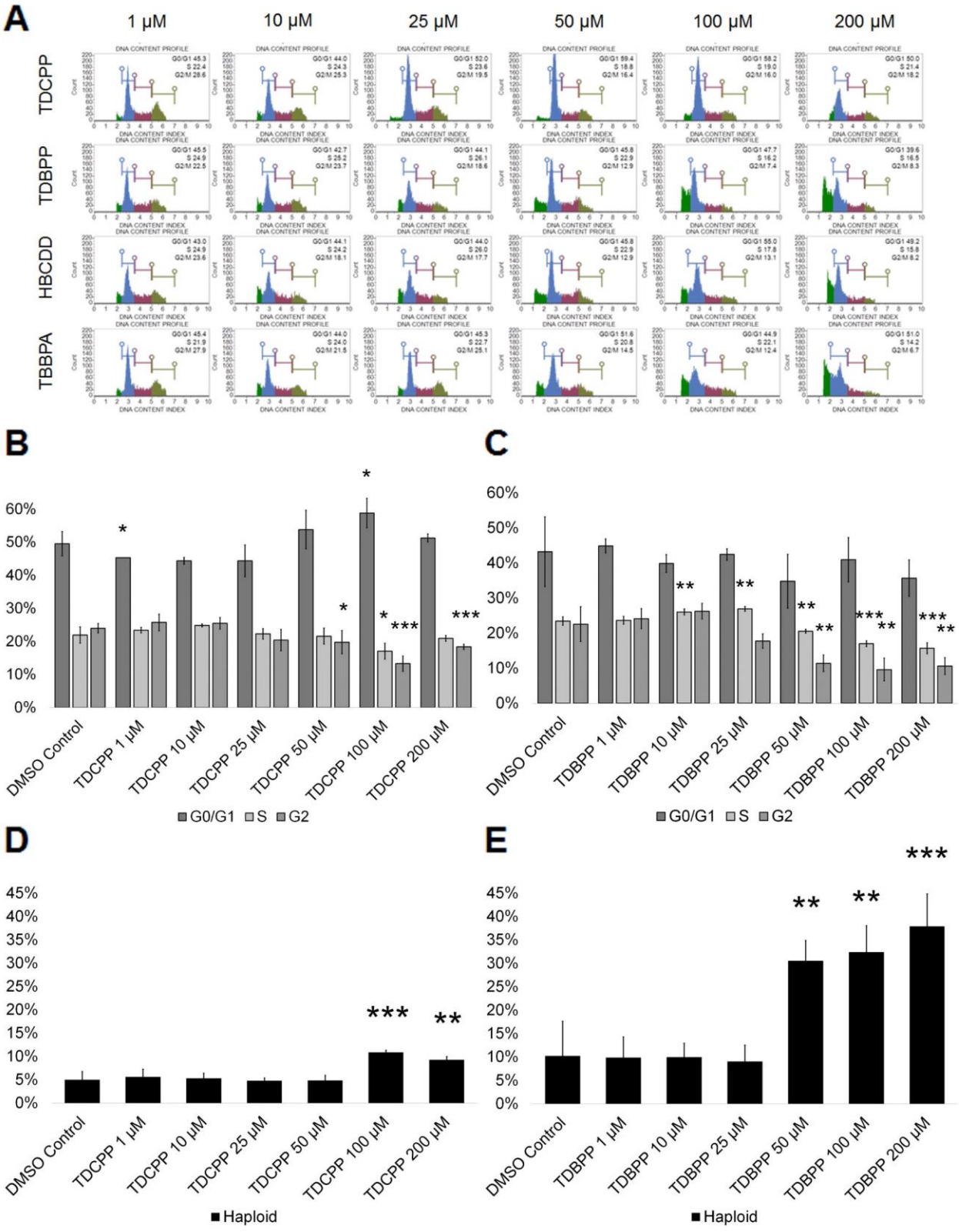
A
1 μM
10 μM
25 μM
50 μM
100 μM
200 μM
TDCPP
TDBPP
HBCDD
TBBPA
B
C
DMSO Control
TDCPP 1 μM
TDCPP 10 μM
TDCPP 25 μM
TDCPP 50 μM
TDCPP 100 μM
TDCPP 200 μM
TDBPP 1 μM
TDBPP 10 μM
TDBPP 25 μM
TDBPP 50 μM
TDBPP 100 μM
TDBPP 200 μM
G0/G1
S
G2
D
E
Haploid

Figure S4. Related to Figure 4. TDCPP, TDBPP, HBCDD, and TBBPA affect the cell cycle in spermatogenic cells derived from hESCs without impacting haploid cell production. (A) Flow cytometry analyses of cell cycle profiles following acute twenty-four hour treatment. Green, blue, purple, and beige populations on flow cytometry correspond to haploid, G0/G1, S, and G2 phases, respectively. (B-C) Graphical representation showing that TDCPP and TDBPP affect the cell cycle of actively dividing hESCS differentiated in *in vitro* spermatogenic conditions. (D-E) Graphical representation showing that TDCPP and TDBPP exposure increases the percentage of haploid cells in spermatogenic cells derived from hESCs. 5,000 events were analyzed, with five replications performed for each condition. Significant changes in percentages of haploid cells and cells in G0/G1, S phase, and G2 were determined using a 1-way analysis of variance (1-way ANOVA) and validated via a Student's t-test, where * is $p<0.05$, ** is $p<0.01$, and *** is $p<0.001$. Data are represented as mean ± SEM.

Impacts of HBCDD and TBBPA Exposure on Spermatogenesis

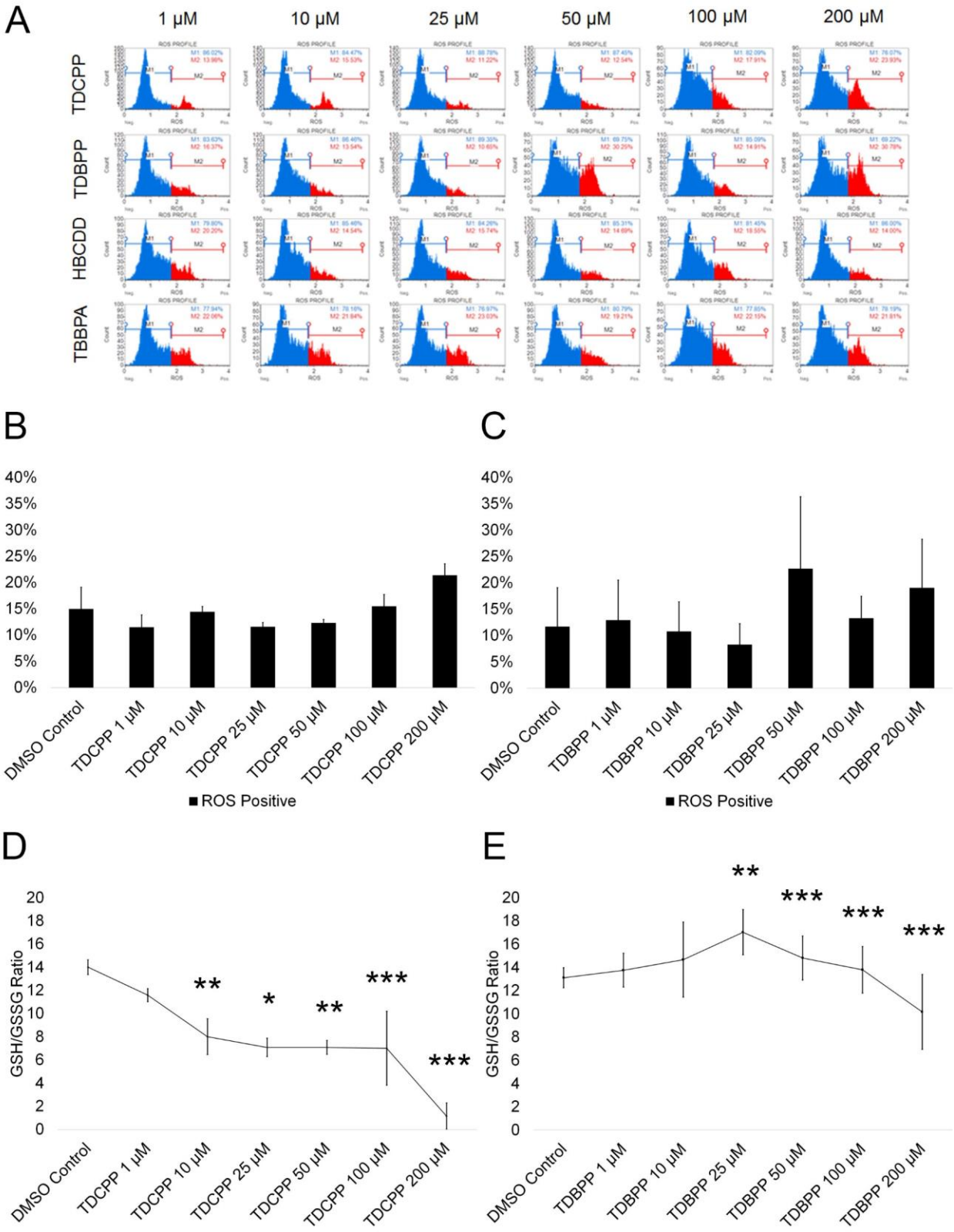

Figure S5. Related to Figure 5. TDCPP, TDBPP, HBCDD, and TBBPA impact ROS production and GSH/GSSG ratios. (A) Flow cytometry analyses indicating percent ROS- and ROS+ cells for all concentrations of TDCPP, TDBPP, HBCDD, and TBBPA assessed. ROS- cells are labeled blue. ROS+ cells are labeled red. (B-C) Graphical representation showing that TDCPP and TDBPP do not overwhelmingly increase ROS+ cells in hESCs differentiated in *in vitro* spermatogenic conditions. (D-E) Graphical representation showing that TDCPP and TDBPP decrease the GSH/GSSG ratio of hESCs differentiated in *in vitro* spermatogenic conditions. 5,000 events were analyzed, with three replications performed for each condition for A-C. Three replications were performed for each condition for D-E. Significant changes in ROS generation and GSH/GSSG ratio were determined using a 1-way analysis of variance (1-way ANOVA) and validated via a Student's t-test, where * is $p<0.05$, ** is $p<0.01$, and *** is $p<0.001$. Data are represented as mean ± SEM.

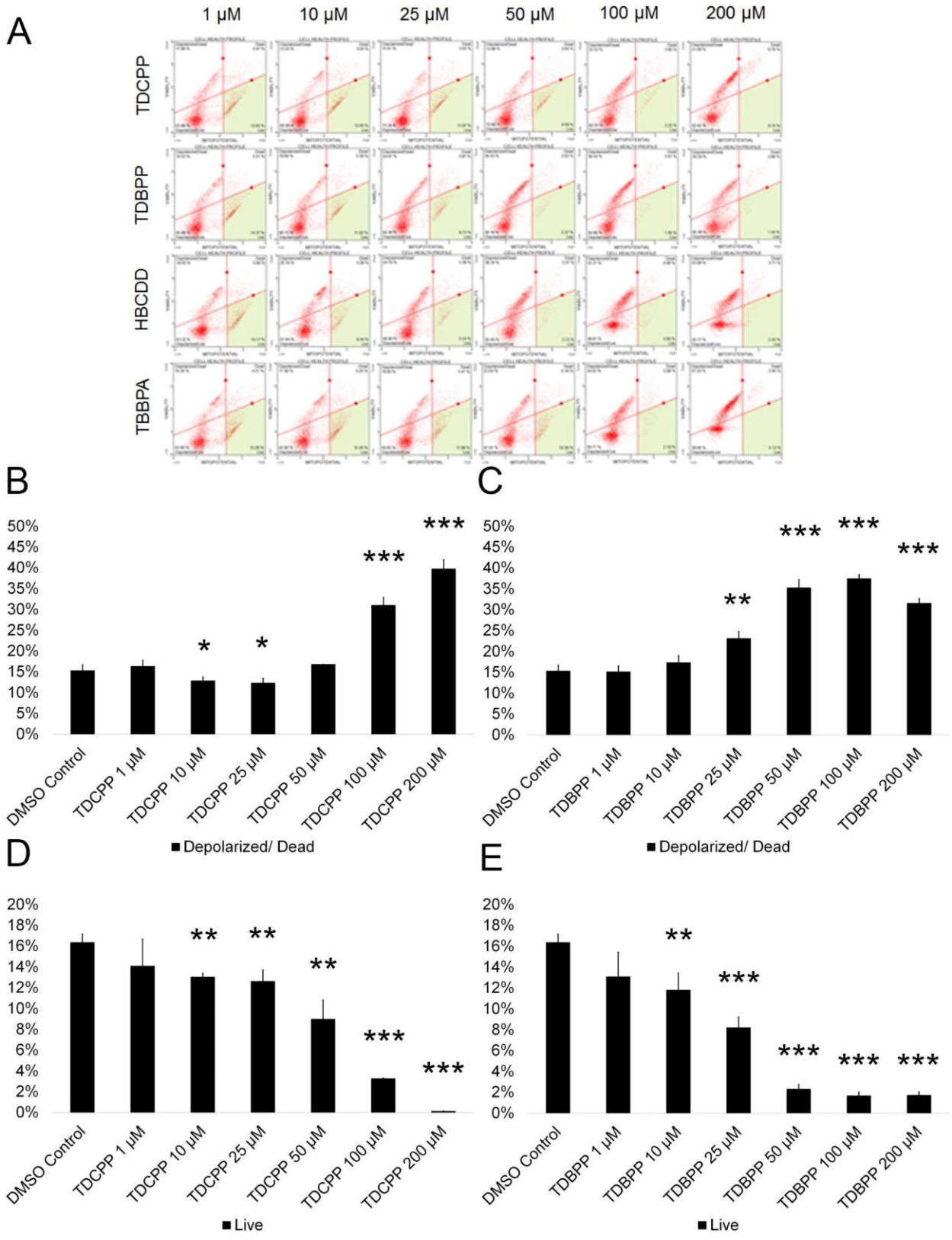
A
1 μM
10 μM
25 μM
50 μM
100 μM
200 μM
TDCPP
TDBPP
HBCDD
TBBPA
B
50%
45%
40%
35%
30%
25%
20%
15%
10%
5%
0%
*
*
***
***
DMSO Control
TDCPP 1 μM
TDCPP 10 μM
TDCPP 25 μM
TDCPP 50 μM
TDCPP 100 μM
TDCPP 200 μM
Depolarized/ Dead
C
**
***
***
***
DMSO Control
TDBPP 1 μM
TDBPP 10 μM
TDBPP 25 μM
TDBPP 50 μM
TDBPP 100 μM
TDBPP 200 μM
Depolarized/ Dead
D
20%
18%
16%
14%
12%
10%
8%
6%
4%
2%
0%
**
**
**
***
***
DMSO Control
TDCPP 1 μM
TDCPP 10 μM
TDCPP 25 μM
TDCPP 50 μM
TDCPP 100 μM
TDCPP 200 μM
Live
E
**
***
***
***
***
DMSO Control
TDBPP 1 μM
TDBPP 10 μM
TDBPP 25 μM
TDBPP 50 μM
TDBPP 100 μM
TDBPP 200 μM
Live

Figure S6. Related to Figure 6. TDCPP, TDBPP, HBCDD, and TBBPA decrease mitochondrial membrane potential and the percentage of healthy, live cells in *in vitro* spermatogenic cultures.. (A) Flow cytometry analyses indicating percent live cells, percent a depolarized/live cells, percent depolarized/dead cells, and percent dead cells. Lower right quadrant represents viable cells, lower left quadrant represents depolarized/live cells, upper right quadrant is depolarized/dead cells, and the upper right quadrant is dead cells. (B-C) Graphical representation showing that TDCPP and HBCDD increase membrane depolarization and death in hESCS differentiated in *in vitro* spermatogenic conditions. (D-E) Graphical representation showing that TDCPP and TDBPP decrease the percentage of healthy, live cells in in hESCS differentiated in *in vitro* spermatogenic conditions. 5,000 events were analyzed, with three replications performed for each condition. Significant changes in mitochondrial potential and live cells were determined using a 1-way analysis of variance (1-way ANOVA) and validated via a Student's t-test, where * is $p<0.05$, ** is $p<0.01$, and *** is $p<0.001$. Data are represented as mean ± SEM.

TRANSPARENT METHODS

CONTACT FOR REAGENT AND RESOURCE SHARING

Further information and requests for resources and reagents should be directed to and will be fulfilled by the Lead Contact, Dr. Charles A. Easley IV (cae25@uga.edu). As per agreement with WiCell Stem Cell Bank, NIH-approved WA01 male hESCs must be obtained directly from WiCell. STO feeder cells required for *in vitro* spermatogenic differentiation can be obtained through the MMRRC.

EXPERIMENTAL MODEL AND SUBJECT DETAILS

Cell culture of H1 ESCs

NIH-approved WA01 (H1, WiCell, Madison, WI) male hESCs were cultured and maintained in mTeSR1 (STEMCELL Technologies, Vancouver, Canada) on matrigel (Corning Life Sciences, Tewksbury, MA) as previously described (Easley et al., 2012). Cell authentication was performed by WiCell but validated by the Easley lab. Markers for pluripotency (Oct4, Sox2, Nanog, SSEA4, TRA-1-60, and TRA-1-81) were examined by immunocytochemistry. Routine karyotyping to ensure proper chromosomal content and lack of translocation was performed every 4-6 months through WiCell's karyotyping core service.

METHOD DETAILS

Differentiation and chemical treatment of H1 ESCs

Direct differentiation into spermatogenic lineages was performed as described (Easley et al., 2012, Easley et al., 2015). Briefly, differentiating cells were maintained on mitomycin C-inactivated mouse STOs in mouse spermatogonial stem cell (SSC) medium containing the following (all from MilliporeSigma, St. Louis, MO, unless noted): MEMalpha (Invitrogen, Waltham, MA), 0.2% Bovine Serum Albumin, 5 µg/ml insulin, 10 µg/ml transferrin, 60 µM putrescine, 2 mM L-glutamine (Invitrogen, Waltham, MA), 50 µM β-mercaptoethanol, 1 ng/ml hbFGF (human basic fibroblast growth factor, PeproTech, Rocky Hill, NJ), 20 ng/ml GDNF (glial-derived neurotrophic factor, PeproTech, Rocky Hill, NJ), 30 nM sodium selenite, 2.36 µM palmitic acid, 0.21 µM palmitoleic acid, 0.88 µM stearic acid, 1.02 µM oleic acid, 2.71 µM linoleic acid, 0.43 µM linolenic acid, 10 mM HEPES, and 0.5X penicillin/streptomycin (Invitrogen, Waltham, MA) for ten days. Media changes occurred every two days. On day nine of the differentiation, cells were treated with 1 µM, 10 µM, 25 µM, 50 µM, 100 µM, and 200 µM of HBCDD (MilliporeSigma, St. Louis, MO) and TBPPA (Tokyo Chemical Industry Co., Ltd. (TCI), Portand, OR) for twenty-four hours. HBCDD and TBBPA were dissolved in dimethyl sulfoxide (DMSO) to create 100 mM stock solutions for use. Cells were collected on day 10 using TrypLE™ Express (Thermofisher, Waltham, MA).

Cell viability and apoptosis

Cell viability was assessed by measuring the percent of apoptotic cells in our cultures using the Muse® Annexin V and Dead Cell Assay Kit (MilliporeSigma, Billerica, MA) by staining with Annexin V and 7-AAD as per manufacturer's instructions to prepare samples for flow cytometry. Samples were run on the Muse® benchtop flow cytometer (MilliporeSigma, Billerica, MA). For each flow cytometry-based experiment, 5,000 events were analyzed for five replications. Cell viability results were verified using the Promega ApoTox-Glo™ Triplex Assay (Promega, Madison, WI) by staining with GF-AFC substrate and bis-AAF-R110 substrate as per manufacturer's instructions. Samples were assessed in triplicate using the Promega GloMax® Explorer (Promega, Madison, WI).

Mitochondrial membrane potential

Mitochondrial membrane potential was assessed by the Muse® MitoPotential Kit (MilliporeSigma, Billerica, MA) by staining with a supplied cationic, lipophilic dye and 7-AAD as per manufacturer's instructions to prepare samples for flow cytometry. Samples were run on the Muse® benchtop flow cytometer (MilliporeSigma, Billerica, MA). For each flow cytometry-based experiment, 5,000 events were analyzed for three replications. Time points collected at 0.5 hr., 1.5 hr., 3 hr., 6 hr., 9 hr., and 12 hr. following exposure to 100 μM HBCDD and TBBPA were also performed in triplicate as described.

Reactive oxygen species (ROS) generation

ROS generation was assessed by the Muse® Oxidative Stress Kit (MilliporeSigma, Billerica, MA) by staining with dihydroethidium as per manufacturer's instructions to prepare samples for flow cytometry. Samples were run on the Muse® benchtop flow cytometer (MilliporeSigma, Billerica, MA). For each flow cytometry-based experiment, 5,000 events were analyzed for three replications. ROS results were verified using the Promega GSH/GSSG-Glo™ Assay (Promega, Madison, WI) as per manufacturer's instructions. Samples were assessed in triplicate using the Promega GloMax® Explorer (Promega, Madison, WI). Time points collected at 0.5 hr., 1.5 hr., 3 hr., 6 hr., 9 hr., and 12 hr. following exposure to 100 μM HBCDD and TBBPA were performed in triplicate utilizing the Muse® Oxidative Stress Kit.

***l*-Sulforaphane Rescue**

l-Sulforaphane (Sigma-Aldrich, St. Louis, MO) rescue of ROS mediated cell death was performed by treating cells with 1 μM *l*-sulforaphane for twelve hours prior to chemical treatment. Cell viability was assessed as described with the Muse® Annexin V and Dead Cell Assay Kit (MilliporeSigma, Billerica, MA). Conditions were performed in triplicate.

Haploid cell production and cell cycle progression

Haploid cell production and cell cycle progression were assessed by generating cell cycle plots revealing haploid cell, G0/G1, S phase, and G2 peaks using the Muse® Cell Cycle Assay Kit (MilliporeSigma, Billerica, MA) by staining with propidium iodide as per manufacturer's instructions to prepare samples for flow cytometry. Samples were run on the Muse® benchtop flow cytometer (MilliporeSigma, Billerica, MA). For each flow cytometry-based experiment, 5,000 events were analyzed for five replications. Haploid peaks were analyzed using guavaSoft™ 3.1.1 (MilliporeSigma, Billerica, MA).

Spermatogonial cell lineage markers

PLZF (promyelocytic leukemia zinc finger, R&D System, Minneapolis, MN) and HILI (piwi like RNA-mediated gene silencing 2, Abcam, Cambridge, MA) immunostaining was performed as previously described (Easley et al., 2012). Briefly, cells were stained with 1.25 μg/mL PLZF or 2.25 μg/mL HILI following fixation with 4% paraformaldehyde and blocking with 4% bovine serum albumin (BSA) in 0.1% Triton X. High content imaging of differentiated hESCs was performed on the ThermoFisher Cellomics ArrayScan® VTI (Thermofisher, Waltham, MA). Quantitative analyses for average PLZF+ and HILI+ total colony area and average total intensity of PLZF+ and HILI+ staining per colony were determined using HCS Studio™ 2.0 Cell Analysis Software included with the ArrayScan® suite. Five replications were performed per condition, with three replications performed for PLZF and HILI recovery assays assessing 100 μM HBCDD and TBBPA exposure. Results were validated via qRT-PCR for PLZF and HILI mRNA transcripts using the Bio-

Rad CFX Connect™ Real-Time PCR Detection System (Bio-Rad, Hercules, CA; see Figure S2 and S3). Two separate replications were performed in duplicate (n=4) for qRT-PCR data. Significant changes in qRT-PCR data were determined using Bio-Rad CFX Manager™ Software (Bio-Rad, Hercules, CA).

QUANTIFICATION AND STATISTICAL ANALYSIS

Significant differences in samples were determined using a 1-way analysis of variance (1-way ANOVA) and validated via a Student's t-test, where * is $p<0.05$, ** is $p<0.01$, and *** is $p<0.001$. Significance for all experiments performed is considered $p \leq 0.05$. For PLZF and HILI immunostaining, n=5 (>50 colonies/well) wells was analyzed for each condition, with n=3 wells analyzed for recovery assays. n=5 replications (wells) were performed for each condition for the Muse® Annexin V and Dead Cell assay and the Muse® Cell Cycle assay, with 5,000 events (cells) collected per replication. n=3 replications were performed for each condition for the Muse® Oxidative Stress assay, the Muse® MitoPotential assay, and the Annexin V and Dead Cell assay following *l*-sulforaphane rescue, with 5,000 events collected per replication. n=3 wells were analyzed for each condition using the Promega GSH/GSSG-Glo™ Assay and the Promega ApoTox-Glo™ Triplex Assay. Two separate replications were performed in duplicate (n=4) for qRT-PCR data. Significant changes in qRT-PCR data were determined using Bio-Rad CFX Manager™ Software. Statistical results are described in the "Results" section as well as figures and figure legends.